Radiometry performance of the VGOS receivers of the Onsala twin telescopes

Gunnar Elgered, Peter Forkman, Rüdiger Haas, and Eskil Varenius

Chalmers University of Technology, Onsala Space Observatory, SE-439 92 Onsala, Sweden

1. Introduction

A fundamental difference when using a stand alone water vapour radiometer (WVR) for calibration or assessment of the wet delays in geodesy VLBI is the different air mass sampled by the telescope and the WVR (see Fig. 1). Petrachenko et al. (2009) suggested to use the VGOS receiver also as a radiometer to observe the sky emission simultaneously with the VLBI source provided that the observed frequency was close enough to the water vapour emission line at 22 GHz.

A simulation study was performed by Forkman et al. (2021) in order to estimate the accuracy of the estimated wet delay as a function of one observed frequency. Fig. 2 summarise the results presented as the expected standard deviation (SD) for three different levels of white noise of the observed sky temperature. These results are representative for cloud-free conditions. When clouds with liquid water content are present there is a need to observe the sky emission at two different frequencies. The simulated corresponding results are presented in Fig. 3.

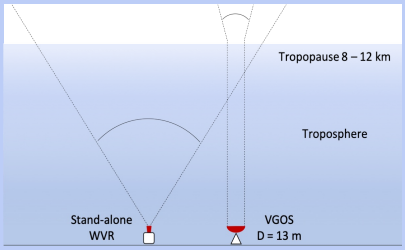

Figure 1. The geometry of the sensed atmosphere.

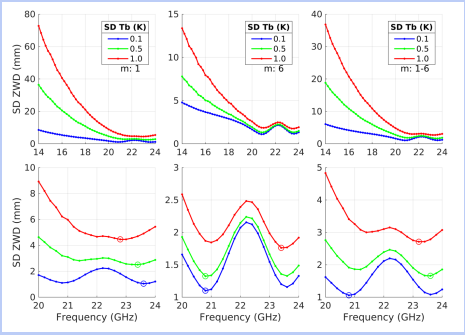

Figure 2. The expected accuracy in the equivalent zenith wet delay (ZWD). Left: 1 airmass, middle: 6 airmasses, and right: 1–6 airmasses. The lower plots zoom in on the frequency range giving the lowest SD. The circles mark the lowest SD at the optimal frequency.

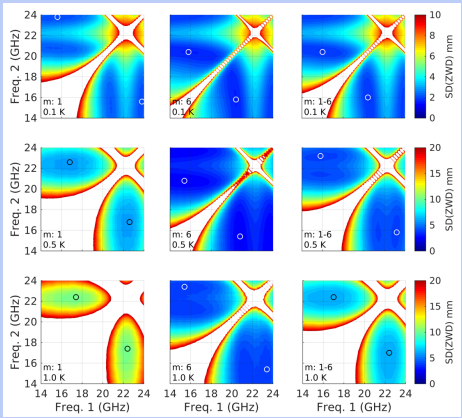

Figure 3. The expected ZWD rms error (SD) for a two-frequency algorithm (one frequency at each axis in the graphs) for 1 (left), 6 (middle) and 1–6 (right) airmasses. The receiver noise is simulated as 0.1 K (top), 0.5 K (middle), and 1.0 K (bottom) for each row. The white areas correspond to rms errors larger than the upper limit of the scale and the circles mark the lowest rms error obtained for the optimal frequency pair.

2. Observations with VGOS receivers

The twin telescopes are equipped with different receivers. The northeast telescope (OE) has a QRFH feed and the southwest telescope (OW) an Eleven feed (see Fig. 4). Fig. 5 depicts the receiver noise temperatures measured using the Y-factor method. For more details of the OTT receivers see Pantaleev et al. (2017).

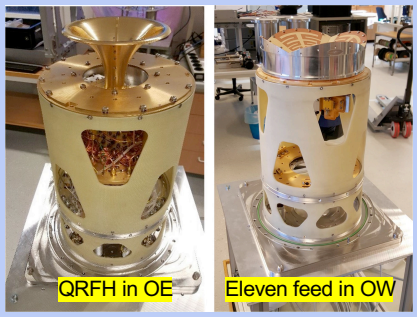

Figure 4. Receivers in the twin telescopes.

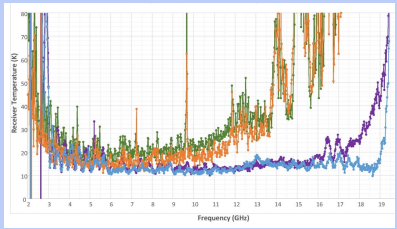

Figure 5. Lab measurements of the receiver temperatures, OE: blue/purple and OW: orange/green.

Data sets

- OW was used from 28 February to 2 March 2023. Elevation angles: 8, 20, and 90 degrees.
- OE was used from 8 to 12 May 2023. Elevation angles: 10, 20, and 90 degrees.

Measurement sequence

The system temperature was measured every 1 s for 1 min at the three different elevation angles. Measurements were carried out in 8 frequency bands, 32 MHz wide, from 15,344 to 15,600 GHz and for both polarizations. The mean value was calculated for each channel for every 1 min period. Because of intermittent interference the value was ignored if the SD was > 1 K (1.5 K at the lowest elevation angle to allow for more atmospheric variability). Thereafter, the mean value of all 16 channels was calculated, and for every 3 min period a tip curve analysis was used to estimate the equivalent zenith sky brightness temperature and the receiver temperature.

Stand-alone WVR Konrad

In order to assess the quality of the estimated sky brightness temperatures and the ZWD from VGOS we used the 20.64 GHz channel of the Konrad WVR. The second channel, used for correction of liquid water in the atmosphere was not used, or needed, because both data sets were acquired during conditions without water clouds.

3. Results

The system temperatures at the three elevation angles are shown in Fig. 6. The larger scatter in Feb–Mar with OW is expected, given the higher system temperatures and perhaps less stable receiver (see Fig. 5).

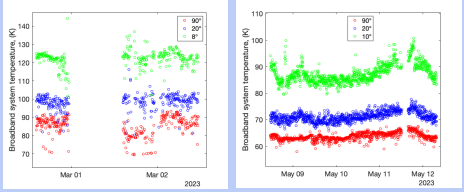

Figure 6. Average system temperature over 1 min and over the 16 frequency bands (both polarizations) from Feb–Mar (OW left) and May (OE right).

3. Results (continued)

Every 3 min interval resulted in an estimated receiver temperature (not shown) and an equivalent zenith sky brightness temperature together with the Konrad WVR temperature (Fig. 7).

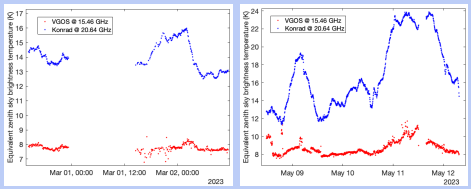

Figure 7. Zenith sky brightness temperatures, (Feb–Mar (OW left) and May (OE right).

The equivalent ZWD are presented in Fig. 8. They were obtained as described by Forkman et al. (2021). We speculate that the large positive offset seen in the ZWD between VGOS and Konrad may be due to an increased ground noise pick up by VGOS with a decreasing elevation angle.

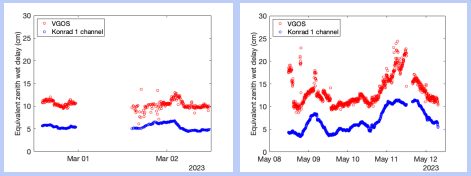

Figure 8. Zenith wet delays, Feb–Mar (OW left) and May (OE right).

Table 1 summarize the ZWD comparison between the stand-alone WVR Konrad and estimates from the VGOS receivers. Statistics are shown for the two complete sessions (black) and for one selected period from each session (red) when the VGOS receivers were more stable.

When the biases are removed we observe standard deviations of the differences of the order of 0.4 cm for a selected period in Feb when the atmosphere was stable, and 1.6 cm for a more variable period in May. This is roughly in agreement with the simulations in Fig. 2. It is clear that the accuracy of wet delay estimates from the VGOS observations after the geodetic processing is normally much higher.

Table 1. ZWD comparison VGOS–Konrad WVR

Time period	Bias (cm)	Standard deviation (cm)	Correlation coefficient
28 Feb–3 Mar (OW)	4.9	0.90	0.42
28 Feb (OW)	5.2	0.37	0.84
8–13 May (OE)	6.3	2.1	0.73
10–13 May (OE)	5.9	1.6	0.87

4. Conclusions and future work

We conclude that even a frequency as low as 15 GHz can provide radiometric information about the wet delay, but it requires a careful screening of the data for receiver instabilities and interferences.

However, observations at 15 GHz are too far away from the water vapour emission line in order to be useful for an assessment of the ZWD estimates from standard VGOS geodetic processing.

Future VGOS radiometry at higher frequencies will still require improvements in the stability and the calibration of the receiver noise temperature.

References

Forkman P, Flygare J, and Elgered G (2021). Water vapour radiometry in geodetic very long baseline interferometry telescopes: assessed through simulations, *J. Geod.*, 95:117, https://doi.org/10.1007/s00190-021-01571z

Pantaleev M, Helldner L, Haas R, et al. (2017). Design, implementation and tests of the signal chain for the twin telescopes at Onsala Space Observatory, Proc. of the 23rd European VLBI Group for Geodesy and Astrometry Working Meeting, eds. R Haas and G Elgered, Gothenburg, pp. 15-19.

Petrachenko B, Niell A, Behrend D et al. (2009). Design aspects of the VLBI2010 system. In: Progress report of the IVS VLBI2010 committee, NASA/TM-2009-214180.